ACS OMEGA

Open Access

http://pubs.acs.org/journal/acsodf

Article

Mechanical Behavior and Indentation-Induced Injury of Soft Microtissues with Different Densification Levels

Wenjuan Zhu, Xiaoning Han, Linhong Deng,* and Xiang Wang*

Cite This: *ACS Omega* 2025, 10, 19675−19681

Read Online

ACCESS | Metrics & More | Article Recommendations

ABSTRACT: Tissue densification is a fundamental biological process involved in development, regeneration, and disease, significantly influencing tissue mechanics and cellular mechanical microenvironments. However, the effects of tissue densification on mechanical properties, the roles of key cytoskeletal components, and their responses to external mechanical stress remain poorly understood. In this study, fibroblast−collagen microtissues were cultured on polydimethylsiloxane (PDMS) microstring scaffolds with different mechanical constraints to generate low- and high-densification microtissues. High-precision indentation force sensor analysis demonstrated that increased densification enhanced microtissue stiffness, accelerated stress relaxation, and elevated energy dissipation. Pharmacological disruption of cytoskeletons revealed the critical role of F-actin in regulating stiffness and viscoelastic resistance in a densification-dependent manner: in high-densification microtissues, F-actin had a greater impact on stiffness and dissipated energy, but a reduced effect on stress relaxation. Furthermore, under 50% strain indentation, high-densification microtissues exhibited irreversible deformation and increased cellular injury. Injured regions showed reduced stiffness, shorter stress relaxation time constants, and higher energy dissipation, indicating structural and cellular damage. These results enhance our understanding of tissue mechanobiology by elucidating the interplay between tissue densification, cytoskeletal mechanics, and injury responses, providing valuable insights for optimizing tissue mechanical microenvironments and improving the mechanical compatibility of biomaterials.

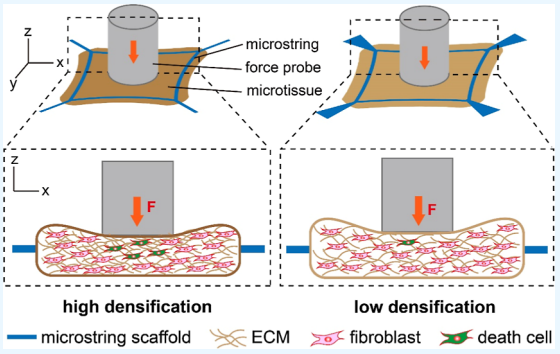

1. INTRODUCTION

Tissue densification is a fundamental biological process involved in embryonic development, tissue regeneration, and pathological conditions like fibrosis and tumors.[1−5] In addition, controlling hydrogel densification is essential for ensuring mechanical compatibility in tissue engineering and regenerative medicine.[6−8] The tissue densification process arises from cellular contractile forces and their interactions with the extracellular matrix (ECM), coupled with the accumulation of ECM proteins. These dynamics lead to increased tissue density and altered mechanical properties, including stiffness, viscoelasticity, and mechanical response, all of which significantly impact tissue structure and function.[6] Various biophysical techniques, including parallel plate pressurization, micropipette aspiration, deformable inclusions, and elastic spring-like force sensors, have been developed to characterize tissue mechanical properties.[6,9,10] Despite these advancements, the role of cells in modulating stress−strain relationships across different densification levels remains underexplored.[11] Addressing these knowledge gaps is essential for elucidating the mechanobiological mechanism underlying tissue densification.

Tissues with varying densification experience diverse mechanical stimuli, including compressive stress, which is prevalent in growth, injury, and disease. Stresses arise internally from movement, organ contraction, and fluid dynamics, while external sources include gravity and applied pressures.[6] Physiological compressive stress supports tissue development, promoting bone growth, muscle expansion, and organ morphogenesis.[10,12−14] Excessive compressive stress, however, can cause tissue injuries, such as necrosis, cartilage degradation, and damage to surrounding structures.[15,16] However, the impact of densification on the mechanical responses of cellular and tissues to compressive stress is poorly characterized, largely due to the limitations of traditional models in simulating densification and applying controlled stress. While animal models provide valuable insights, dynamic and complex in vivo conditions make mechanical measurements challenging.[9] Similarly, 3D cell culture systems, including spheroids and organoids, offer important perspectives on tissue behavior but

Received: January 21, 2025
Revised: March 11, 2025
Accepted: April 30, 2025
Published: May 6, 2025

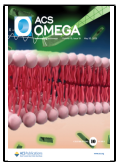

lack precise control over densification and feature non-physiological boundary conditions.[17] As a result, critical aspects like stress distribution, cell death patterns, and changes in mechanical properties under compressive stress remain unclear.

To address these challenges, microtissue systems based on fibroblasts−collagen matrix contraction offer a promising solution. Fibroblasts play a pivotal role in the densification process by generating contractile forces and secreting ECM components.[18,19] Collagen not only ensures structural integrity but also serves as the primary substrate for physical and chemical interactions with cells.[20] By integrating micronano fabrication technology, these systems enable precise control over mechanical constraints at the millimeter scale, facilitating multiscale mechanobiological studies.[21,22] Building on these advances, we developed a soft microtissue model cultured on square microstring scaffolds, where tissue densification was modulated by scaffold elasticity. High-precision indentation force sensors were used to assess the mechanical responses of microtissues with different densification levels. The contribution of the cytoskeleton to microtissue mechanics was systematically evaluated. Furthermore, using this system as a scaled-down model, we investigated the effects of densification on cell viability and the mechanical properties of microtissues subjected to indentation-induced injury. The results reveal the mechanical behavior and damage responses of soft microtissues with different densification levels, providing valuable insights from the perspective of densification mechanobiology to optimize tissue engineering approaches and advance the design of mechanically compatible biomaterials.

2. MATERIALS AND METHODS

2.1. Fabrication of Microstring Scaffolds. Two types of microstring scaffolds were designed using LayoutEditor software (Juspertor, Germany). Each scaffold consists of a square microstring (length = 2.4 mm) to support microtissue growth. To control the densification level of the microtissues, the support strings anchoring the corners of the square were designed with different widths. A silicon master containing scaffold patterns (height = 50 μm, width = 100 μm) was fabricated via deep reactive ion etching (Suzhou Wenhao, China). A polydimethylsiloxane (PDMS) negative mold was prepared by casting a 10:1 (v/v) mixture of Sylgard 184 elastomer and curing agent (Dow Corning, USA) onto the silicon master. The patterned mold surface was treated with oxygen plasma (PT-5S, Sanhe Boda, China) and coated with 1% poly(vinyl alcohol) (PVA, Aladdin Bio-Chem Technology, China). After air drying, uncured PDMS was poured into the mold and cured at 80 °C for 4 h. Subsequently, four PDMS blocks (height = 2 mm) were bonded to the ends of support strings using uncured PDMS, followed by thermal curing and plasma treatment. A glass coverslip (diameter = 12 mm) was bonded to the opposite side of the PDMS blocks. The PVA coating was dissolved in water to release the scaffold. Finally, a glass support (height = 1.5 mm) was bonded to the glass coverslip beneath the central region of the microstrings to support ungelled collagen.

2.2. Microtissue Preparation and Drug Treatments. Mouse NIH/3T3 fibroblast (American Type Cell Culture, USA) were cultured in Dulbecco's modified Eagle medium (Gibco, Life Tech, USA) supplemented with 10% fetal calf serum (FBS, Gibco) at 37 °C and 5% CO_2. Microtissues were prepared following our previously established protocol.[23] Briefly, scaffolds were secured to the bottom of a 12-well culture plate by gluing the glass coverslip's underside to the plate substrate with silicone grease (Baysilone, GE, USA) to ensure stability. Cultured 3T3 cells were trypsinized, and mixed with neutralized rat tail type I collagen (Advanced Biomatrix, USA) to a final concentration of 10^6 cells/mL in 2 mg/mL collagen solution. A 20 μL mixture was placed at the scaffold's center and incubated at 37 °C for 40 min to allow polymerization. To evaluate the role of cellular activity in the mechanical response of microtissues, microtissues were incubated for 3 h with 10 μM cytochalasin D, 5 μM blebbistatin, 10 μM nocodazole, or 0.5% Triton X-100 (all from Sigma-Aldrich, USA) before force measurements.

2.3. Experimental Setup and Imaging. A microindentation system (MicroTouch, Suzhou Nators, China) was used to assess the mechanical properties of microtissues. The system includes a force-sensing probe with a round stainless steel tip (diameter = 800 μm) capable of measuring reaction forces with a resolution of 0.5 μN. The probe was mounted on a three-axis motion stage, enabling precise vertical movement with a resolution of 5 nm. Displacement and force data were recorded at a sampling rate of 50 Hz using the software provided by the manufacturer. The microindentation system was integrated with a motorized stage (Prior Scientific, USA) on a Zeiss Axio Observer 7 fluorescence microscope (Carl Zeiss MicroImaging, Germany), equipped with 5×/0.16 NA and 20×/0.5 objectives, and an ORCA-Flash4.0 camera (Hamamatsu, Japan). Bright-field live-cell imaging was recorded by the ZEN software (Carl Zeiss MicroImaging) 1 h after cell seeding.

2.4. Force Measurements. Samples were incubated in a medium supplemented with 20 mM HEPES (Sigma-Aldrich) and placed in the microscopy stage. Guided by the microscope, the force probe tip was positioned 10 to 20 μm above the microtissue surface. The probe was then moved toward the sample in 2 μm steps using the micromanipulator until contact was detected, indicated by a consistent change in measured force (typically within 5 μm of displacement after the initial force change). Then, the probe indented the sample at a continuous rate of 2 μm/s to a depth of 75 μm for high-densification samples or 90 μm for low-densification samples, ensuring a consistent strain of 50% for both types of microtissues. Force−time or force−displacement data were recorded using the system's software.

To evaluate viscoelastic properties, stress relaxation experiments were conducted with the 800 μm force probe. Indentation depth was increased in 10 μm increments, with each step held for 30 s. Relaxation time constants (τ) were calculated using Origin 2024 software (OriginLab, USA) by fitting an exponential decay model to the obtained stress relaxation curves: $\sigma(t) = \sigma_0\, e^{-t/\tau} + \sigma_\infty$, where $\sigma(t)$ represents the stress at time t. Energy dissipation during mechanical loading was evaluated using cyclic loading−unloading tests. Microtissues were subjected to loading and unloading at a velocity of 2 μm/s to a strain of 50%. The hysteresis loop was recorded using the system's software. Relative energy dissipation (W) was calculated as $W = (S_{load} - S_{unload})/S_{load}$, where S_{load} and S_{unload} represent the absorbed energy during loading (area under the loading curve) and the recovered energy during unloading (area under the unloading curve), respectively.

2.5. Microtissue Injury and Cell Viability Assay. For indentation-induced injury experiments, microtissues cultured

https://doi.org/10.1021/acsomega.5c00639
ACS Omega 2025, 10, 19675−19681

for 48 h were indented at the center to a strain of 20% or 50% for 1 h using the force probe. Samples were then incubated for an additional 24 h before force measurements and cell viability assays. Cell viability was evaluated using a calcein-AM/propidium iodide (PI) double-stain kit (Solarbio Science & Technology, China). Following incubation, the medium was replaced with a staining buffer containing 2 μM calcein-AM, 1 μM PI, and 1 μM Hoechst 33342 (Beyotime, China), followed by a 30 min incubation in the dark. Samples were incubated in the dark for 15 min before imaging with a Zeiss 710 confocal microscope equipped with a 20×/0.5 NA objective (Carl Zeiss MicroImaging). Viability was quantified as the ratio of PI-positive cells to the total number of cells labeled with Hoechst 33342.

2.6. Statistical Analysis. All experiments were conducted with at least four independent groups. Student's two-tailed *t*-test and ANOVA were performed to compare the means of two groups and more than two groups, respectively, using Prism 10 (GraphPad, USA). Data are presented as mean ± S.D., with error bars representing 95% confidence intervals. Significance levels were denoted as follows: ns for not significant, * for $P < 0.05$, ** for $P < 0.01$, and *** for $P < 0.001$.

3. RESULTS

3.1. Mechanical Responses of Microtissues with Different Densification Levels. To control microtissue shape and densification levels, two types of square PDMS scaffolds were fabricated, featuring support strings with different widths. Scaffolds with wide support strings provided more constraint at the corners (Figure 1A, upper panel), while

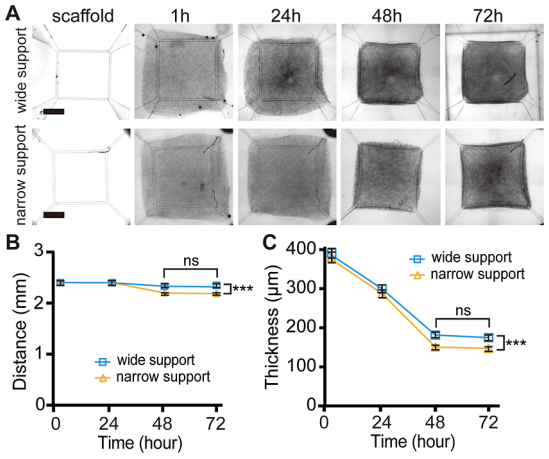

Figure 1. Microtissues with different densification levels. (A) Formation of microtissues with different densification levels on microstring scaffolds. Scale bars = 1.0 mm. (B) Distance between the parallel strings of square scaffolds (n = 12) and (C) thickness of microtissues grown on two types of square scaffolds (n = 24) at indicated culture time.

scaffolds with narrow support strings imposed less constraint (Figure 1A, lower panel). A mixture of type I collagen and 3T3 fibroblasts was pipetted onto the scaffolds and incubated at 37 °C to facilitate collagen polymerization and anchorage. Over 48 h, fibroblasts' contractile forces caused stable microtissue densification, as indicated by the measured distance between parallel strings and microtissue thickness (Figure 1B,C). Additionally, microtissues cultured on narrow-supported scaffolds exhibited greater contraction than those on wide-supported scaffolds. The thickness of the microtissues grown on narrow-supported scaffolds (151 ± 6 μm) was significantly lower than those grown on wide-supported scaffolds (181 ± 6 μm). These observations confirm the successful generation of low-densification microtissues (LD-MTs) and high-densification microtissues (HD-MTs) using scaffolds with different constraints.

To investigate the mechanical properties of these microtissues, a force sensor was used to apply controlled forces to the center of the microtissues and measure their response. Under continuous indentation at a rate of 2 μm/s (~1% strain rate), both LD-MTs and HD-MTs exhibited a linear stress–strain relationship up to 40% strain (Figure 2A). HD-MTs

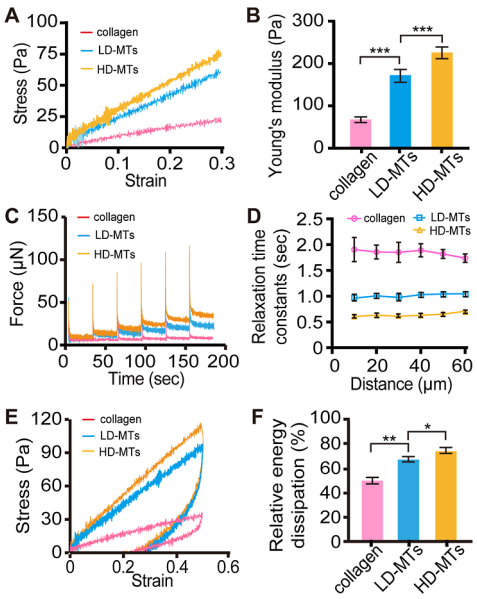

Figure 2. Mechanical properties of microtissues with different densification levels. (A) Stress–strain curves of cell-free collagen, LD-MTs, and HD-MTs under continuous indentation. (B) Young's modulus was calculated from the slopes of the stress–strain curves in (A) (n = 8). (C) Stress relaxation behavior of cell-free collagen, LD-MTs, and HD-MTs under stepwise loading with successive 10 μm displacements. (D) Relaxation time constants as a function of indentation distance (n = 4). (E) Hysteresis behavior of cell-free collagen, LD-MTs, and HD-MTs under uniaxial cyclic loading. (F) Relative energy dissipation during uniaxial cyclic loading (n = 6).

demonstrated higher stress levels at equivalent strain, with a significantly greater Young's modulus (228 ± 14 Pa) compared to LD-MTs (174 ± 14 Pa) (Figure 2B), classifying both as soft tissues. Viscoelasticity, a key mechanical property of soft tissues, was examined by analyzing stress relaxation behavior under stepwise loading. Successive 10 μm displacements were applied to the center of microtissues (Figure 2C). Stress relaxation time constants (τ) were calculated from the stress relaxation curves, revealing significantly faster stress decay in HD-MTs than LD-MTs, regardless of strain level (Figure 2D). This indicates that HD-MTs are more viscosity-dominated, leading to a faster relaxation process. Energy dissipation was further assessed using uniaxial cyclic loading at a strain rate of at strain rates of 2 μm/s (Figure 2E). Quantitative analysis of the hysteresis loops revealed significantly higher relative energy dissipation in HD-MTs compared to LD-MTs (Figure 2F), suggesting greater energy loss but reduced elastic energy

https://doi.org/10.1021/acsomega.5c00639
ACS Omega 2025, 10, 19675−19681

storage capacity in HD-MTs. For comparison, cell-free collagen exhibited a significantly lower Young's modulus, longer stress relaxation time, and reduced energy dissipation compared to microtissues, indicating the key role of the cellular component in shaping the overall mechanical properties of microtissues.

3.2. Role of Cells in Response to Mechanical Loading of Microtissues. To investigate the cellular factors contributing to the mechanical responses of microtissues, we focused on cytoskeleton and actomyosin components, which are critical determinants of cellular forces. Microtissues cultured for 48 h were pretreated with 10 μM cytochalasin D (CytoD) to disrupt actin filaments, 5 μM blebbistatin (Bleb) to inhibit myosin-II activity, 10 μM nocodazole (Noc) to block microtubule polymerization, or 0.5% Triton X-100 to abolish cellular forces. Stress−strain experiments revealed that all treatments significantly reduced Young's modulus of both LD-MTs and HD-MTs (Figure 3A). Among them, CytoD exhibited the most pronounced effect, particularly in HD-MTs, suggesting a prominent role of the actin cytoskeleton in maintaining stiffness in denser tissues.

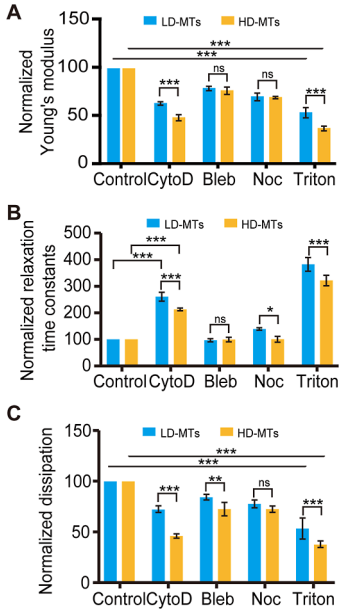

Figure 3. Influence of cytoskeleton on microtissue mechanics. (A) Normalized Young's modulus ($n \geq 5$), (B) normalized relaxation time constants ($n \geq 6$), and (C) normalized energy dissipation ($n = 5$) of LD-MTs and HD-MTs treated with different drugs.

To further elucidate the role of cellular components in regulating the viscoelastic properties of microtissues, we analyzed stress relaxation in drug-treated samples. As shown in Figure 3B, CytoD significantly increased relaxation time constants in both types of microtissues, suggesting that actin filaments are major contributors to viscoelastic resistance. Moreover, the effect of CytoD was more pronounced in LD-MTs compared to HD-MTs. When the energy dissipation of drug-treated microtissues was evaluated, the results showed that all treatments significantly reduced energy dissipation, reinforcing the critical role of the cytoskeleton in energy absorption and dissipation (Figure 3C). CytoD and Bleb treatments had greater effects in HD-MTs than LD-MTs, indicating a prominent role for actomyosin in denser tissues. It should be noted that all measured mechanical properties of microtissues were drastically altered when cells were removed using Triton X-100, emphasizing the critical contribution of cellular components to tissue mechanics. Together, these findings underscore the distinct roles of actin filaments in regulating the viscoelastic and dissipative properties of microtissues, with effects strongly influenced by tissue density.

3.3. Effects of Densification Level on Indentation-Induced Microtissue Injury. To investigate the impact of tissue densification on cell injury caused by indentation, continuous indentation was applied to the central regions of microtissues for 1 h using a force probe, followed by a 24 h recovery period. Morphological analysis revealed that under 20% strain, the thickness of the indented region in both LD-MTs and HD-MTs was significantly reduced 10 min after unloading, but recovered within 24 h (Figure 4A). In contrast, at 50% strain, the thickness of indented regions remained below preloading levels, indicating irreversible plastic deformation and potential tissue damage. We therefore evaluated cell viability in these microtissues. Confocal microscopy imaging showed more cell death in the indented regions of HD-MTs compared to LD-MTs (Figure 4B). Statistical analysis confirmed that cell death rates in the indented regions were significantly higher than those in unindented regions or control microtissues without indentation (Figure 4C). Importantly, HD-MTs exhibited a significantly higher cell death rate (8.7%) compared to LD-MTs (4.4%). This observation indicates that higher densification levels increase the susceptibility of cells to mechanical stress-induced injury, emphasizing the importance of tissue architecture in mechanical injury responses.

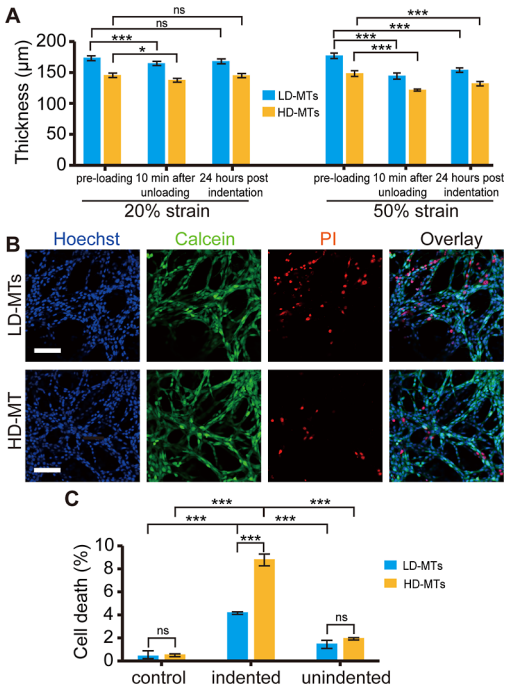

Figure 4. Indentation-induced injury in microtissues. (A) Thickness of the indented region in LD-MTs and HD-MTs before indentation, and at 10 min and 24 h postindentation ($n = 4$). (B) Cell viability in indented regions of LD-MTs and HD-MTs 24 h after 50% strain indentation, assessed using calcein/PI and Hoechst 33342 staining. Scale bars = 100 μm. (C) Cell death rates in LD-MTs and HD-MTs in response to 50% strain indentation ($n = 7$).

https://doi.org/10.1021/acsomega.5c00639
ACS Omega 2025, 10, 19675−19681

3.4. Mechanical Properties of Microtissues Injured by Indentation. To elucidate the impact of mechanical injury on the mechanical properties of microtissues, mechanical measurements were conducted on the indented regions 24 h after applying a 50% strain indentation for 1 h. Young's modulus analysis revealed that, although HD-MTs initially exhibited higher stiffness than LD-MTs in control conditions, both showed a comparable reduction in stiffness following indentation (Figure 5A). This decrease suggests that large-strain deformation caused structural alterations, compromising the load-bearing capacity of the tissues. Additionally, stress relaxation of the indented regions was significantly reduced in HD-MTs compared to LD-MTs (Figure 5B), reflecting greater structural rearrangement and damage in denser tissues. Under cyclic loading conditions, both LD-MTs and HD-MTs exhibited increased energy dissipation in the indented regions (Figure 5C), suggesting enhanced energy loss due to irreversible deformation or accumulated damage. These results highlight the complex interplay between microtissue densification and mechanical behavior under large-strain conditions, underscoring the impact of densification on tissue resilience and injury response.

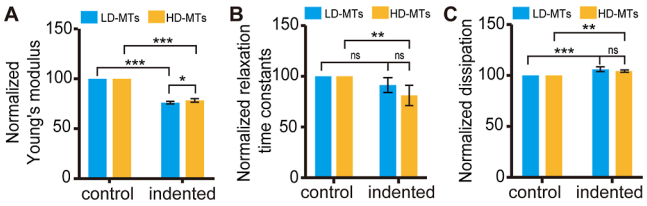

Figure 5. Mechanical properties of indentation-induced regions in microtissues. (A) Normalized Young's modulus (n = 5), (B) normalized relaxation time constants (n = 5), and (C) normalized energy dissipation (n = 4) of the indented regions in LD-MTs and HD-MTs, measured 24 h after 1 h of 50% strain-induced injury.

4. DISCUSSION

Soft tissue development and wound healing often involve transitions from low to high densification.[24] However, studies on the mechanical characteristics of soft tissues at different densification levels, and their responses to compressive stress, remain limited. To address this, we developed a microtissue model on square PDMS scaffolds to control densification. Both LD-MTs and HD-MTs were classified as soft tissues with stiffness ranging between 150 and 250 Pa. This range aligns with the stiffness of soft tissues like brain and adipose tissues, as well as hydrogels used in bioengineering applications.[6,8] Our previous studies demonstrated that cellular forces and collagen matrix tension synergistically drive microtissue densification.[23] Here, we revealed a distinct mechanical contrast between microtissues and cell-free collagen. Building on this, we found that the ECM accounted for approximately half of the stiffness, with the remaining stiffness attributed to cellular components. Among these, actin filaments play a dominant role in preserving tissue stiffness, particularly in LD-MTs. This is likely due to that the ECM in LD-MTs is less dense, providing relatively weaker structural support compared to HD-MTs. As a result, the actin cytoskeleton becomes the primary contributor to tissue stiffness by maintaining cellular shape, resisting deformation, and transmitting intracellular forces.

Through our study of microtissue viscoelasticity, we observed that HD-MTs exhibit shorter stress relaxation time constants and greater dissipated energy, which may be relevant to pathological conditions such as fibrosis, where excessive ECM remodeling leads to tissue stiffening and mechanical dysfunction. This behavior is likely attributed to increased internal friction, noncovalent interactions within the ECM, and stronger intercellular and cellular-matrix connections in denser tissues, which collectively enhance mechanical coupling and delay molecular rearrangement.[25,26] While the influence of ECM viscoelasticity on cellular behavior has been extensively investigated, our findings highlight the critical role of F-actin in regulating tissue viscoelasticity, as evidenced by significantly increased relaxation time constants and reduced dissipated energy after CytoD treatment. These effects are density-dependent: in LD-MTs, where ECM contributions are weaker, F-actin disruption leads to a pronounced increase in relaxation time constant. Conversely, in HD-MTs, F-actin plays a more prominent role in regulating dissipated energy compared to LD-MTs. Thus, F-actin is essential not only for microtissue stiffness but also for modulating viscoelastic properties in a density-dependent manner. The underlying molecular mechanism probably involved integrin-mediated mechanotransduction, which reinforces actomyosin contractility in HD-MTs. In addition, fibroblast-driven collagen remodeling also enhances ECM organization, leading to higher stiffness and faster stress relaxation in HD-MTs.

Understanding cellular and tissue responses to stress in soft mechanical environments is critical, as mechanical compression is commonly encountered in processes such as soft tissue deformation, hydrogel injection, and 3D bioprinting.[27,28] While previous research has established that mechanical loading can lead to cell death, most studies have focused primarily on the effects of external forces, overlooking the influence of the ECM mechanical properties.[29,30] Our results reveal that sustained 50% indentation for 1 h induces plastic deformation in microtissues, persisting even after 24 h, suggesting irreversible ECM deformation.[31,32] Importantly, mechanical stress exacerbates cellular injury in HD-MTs, probably due to a stiffer ECM and enhanced cellular-matrix interactions that concentrate mechanical forces.[33] The underlying mechanisms may involve cell membrane damage and cytoskeleton reorganization.[16,34] Therefore, modulating microtissue densification could be a promising strategy for optimizing cell-laden hydrogel design, ensuring mechanical properties that support cell survival and functional tissue integration. Additionally, biomaterials intended for load-bearing applications (e.g., cartilage repair, 3D bioprinting) should incorporate stress-dissipating elements to prevent excessive cellular damage.

Mechanical characterization of damaged regions showed a significant reduction in stiffness despite decreased thickness, contrasting with higher compressive moduli observed in indented, cell-free collagen surfaces.[20] This discrepancy may arise from fiber buckling and collapse in the plastic deformation zone.[35] Pharmacological treatments further indicated that damaged cells contribute less to tissue stiffness, exacerbating mechanical weakness. Viscoelastic analysis showed density-dependent responses to mechanical damage. In HD-MTs, stress relaxation was significantly reduced, suggesting that denser ECM networks undergo greater structural rearrangement and experience more substantial damage under large-strain deformation. Both LD-MTs and HD-MTs showed increased energy dissipation in indented regions, further suggesting irreversible deformation and

https://doi.org/10.1021/acsomega.5c00639
ACS Omega 2025, 10, 19675−19681

compromised structural integrity following injury. While our fibroblast−collagen microtissue system allows precise control over densification and mechanical measurements, it does not fully replicate the cellular heterogeneity and ECM complexity of native tissues. Future studies should incorporate more complex 3D tissue models to better mimic in vivo conditions and further explore the role of multiple cell types in densification-dependent mechanical behaviors.

5. CONCLUSIONS

This study elucidates the mechanical behaviors of microtissues with different densification levels, highlighting the critical role of F-actin in regulating soft tissue stiffness and viscoelasticity. Increased densification not only induces higher stiffness, faster stress relaxation, and greater dissipated energy but also concentrates mechanical stress, resulting in greater cellular damage. These findings underscore the complex interplay between tissue densification, ECM mechanics, and cellular contributions in shaping tissue behavior. The insights gained from this study deepen our understanding of the mechanobiology of tissue densification, providing valuable guidance for optimizing the mechanical environment in tissue engineering and informing the design of biomaterials with improved mechanical compatibility.

AUTHOR INFORMATION

Corresponding Authors

Linhong Deng − *Institute of Biomedical Engineering and Health Sciences and School of Medical and Health Engineering, Changzhou University, 213164 Changzhou, Jiangsu, China;* orcid.org/0000-0003-1970-8239; Email: dlh@cczu.edu.cn

Xiang Wang − *Institute of Biomedical Engineering and Health Sciences and School of Medical and Health Engineering, Changzhou University, 213164 Changzhou, Jiangsu, China;* orcid.org/0000-0002-4938-010X; Email: wangxiang@cczu.edu.cn

Authors

Wenjuan Zhu − *Institute of Biomedical Engineering and Health Sciences and School of Pharmacy, Changzhou University, 213164 Changzhou, Jiangsu, China*

Xiaoning Han − *Institute of Biomedical Engineering and Health Sciences and School of Medical and Health Engineering, Changzhou University, 213164 Changzhou, Jiangsu, China*

Complete contact information is available at: https://pubs.acs.org/10.1021/acsomega.5c00639

Author Contributions

XW designed the study. WZ and XH performed the experiments. WZ, XH, and XW analyzed the results. XW and LD wrote the manuscript. All authors have read and agreed to the published version of the manuscript.

Funding

This work was supported by the National Natural Science Foundation of China (No. 12472317 to X.W., No. 12272063 to L.D.).

Notes

The authors declare no competing financial interest.

ACKNOWLEDGMENTS

We thank Lei Liu and Yan Pan for their assistance with the confocal experiments.

REFERENCES

(1) Shahbazi, M. N. Mechanisms of human embryo development: from cell fate to tissue shape and back. *Development* **2020**, *147* (14), dev190629.

(2) Sarate, R. M.; Hochstetter, J.; Valet, M.; Hallou, A.; Song, Y.; Bansaccal, N.; Ligare, M.; Aragona, M.; Engelman, D.; Bauduin, A.; et al. Dynamic regulation of tissue fluidity controls skin repair during wound healing. *Cell* **2024**, *187* (19), 5298−5315.e19.

(3) Mao, Y.; Wickstrom, S. A. Mechanical state transitions in the regulation of tissue form and function. *Nat. Rev. Mol. Cell Biol.* **2024**, *25* (8), 654−670.

(4) Tschumperlin, D. J.; Ligresti, G.; Hilscher, M. B.; Shah, V. H. Mechanosensing and fibrosis. *J. Clin. Invest.* **2018**, *128* (1), 74−84.

(5) Winkler, J.; Abisoye-Ogunniyan, A.; Metcalf, K. J.; Werb, Z. Concepts of extracellular matrix remodelling in tumour progression and metastasis. *Nat. Commun.* **2020**, *11* (1), 5120.

(6) Guimarães, C. F.; Gasperini, L.; Marques, A. P.; Reis, R. L. The stiffness of living tissues and its implications for tissue engineering. *Nat. Rev. Mater.* **2020**, *5* (5), 351−370.

(7) Tang, S.; Richardson, B. M.; Anseth, K. S. Dynamic covalent hydrogels as biomaterials to mimic the viscoelasticity of soft tissues. *Prog. Mater. Sci.* **2021**, *120*, 100738.

(8) Blache, U.; Ford, E. M.; Ha, B.; Rijns, L.; Chaudhuri, O.; Dankers, P. Y. W.; Kloxin, A. M.; Snedeker, J. G.; Gentleman, E. Engineered hydrogels for mechanobiology. *Nat. Rev. Methods Primers* **2022**, *2* (1), 98.

(9) Gómez-González, M.; Latorre, E.; Arroyo, M.; Trepat, X. Measuring mechanical stress in living tissues. *Nat. Rev. Phys.* **2020**, *2* (6), 300−317.

(10) Maniou, E.; Todros, S.; Urciuolo, A.; Moulding, D. A.; Magnussen, M.; Ampartzidis, I.; Brandolino, L.; Bellet, P.; Giomo, M.; Pavan, P. G.; et al. Quantifying mechanical forces during vertebrate morphogenesis. *Nat. Mater.* **2024**, *23* (11), 1575−1581.

(11) Krieg, M.; Fläschner, G.; Alsteens, D.; Gaub, B. M.; Roos, W. H.; Wuite, G. J. L.; Gaub, H. E.; Gerber, C.; Dufrêne, Y. F.; Müller, D. J. Atomic force microscopy-based mechanobiology. *Nat. Rev. Phys.* **2019**, *1* (1), 41−57.

(12) Wang, L.; You, X.; Zhang, L.; Zhang, C.; Zou, W. Mechanical regulation of bone remodeling. *Bone Res.* **2022**, *10* (1), 16.

(13) Heisenberg, C.-P.; Bellaïche, Y. Forces in Tissue Morphogenesis and Patterning. *Cell* **2013**, *153* (5), 948−962.

(14) Valet, M.; Siggia, E. D.; Brivanlou, A. H. Mechanical regulation of early vertebrate embryogenesis. *Nat. Rev. Mol. Cell Biol.* **2022**, *23* (3), 169−184.

(15) Gonzalez-Rodriguez, D.; Guillou, L.; Cornat, F.; Lafaurie-Janvore, J.; Babataheri, A.; de Langre, E.; Barakat, A. I.; Husson, J. Mechanical Criterion for the Rupture of a Cell Membrane under Compression. *Biophys. J.* **2016**, *111* (12), 2711−2721.

(16) Valon, L.; Levayer, R. Dying under pressure: cellular characterisation and in vivo functions of cell death induced by compaction. *Biol. Cell* **2019**, *111* (3), 51−66.

(17) Efremov, Y. M.; Zurina, I. M.; Presniakova, V. S.; Kosheleva, N. V.; Butnaru, D. V.; Svistunov, A. A.; Rochev, Y. A.; Timashev, P. S. Mechanical properties of cell sheets and spheroids: the link between single cells and complex tissues. *Biophys. Rev.* **2021**, *13* (4), 541−561.

(18) D'Urso, M.; Kurniawan, N. A. Mechanical and Physical Regulation of Fibroblast−Myofibroblast Transition: From Cellular Mechanoresponse to Tissue Pathology. *Front. Bioeng. Biotechnol.* **2020**, *8*, 609653.

(19) Plikus, M. V.; Wang, X.; Sinha, S.; Forte, E.; Thompson, S. M.; Herzog, E. L.; Driskell, R. R.; Rosenthal, N.; Biernaskie, J.; Horsley, V. Fibroblasts: Origins, definitions, and functions in health and disease. *Cell* **2021**, *184* (15), 3852−3872.

(20) Novak, T.; Seelbinder, B.; Twitchell, C. M.; van Donkelaar, C. C.; Voytik-Harbin, S. L.; Neu, C. P. Mechanisms and Microenvironment Investigation of Cellularized High Density Gradient Collagen Matrices via Densification. *Adv. Funct. Mater.* **2016**, *26* (16), 2617−2628.
(21) Chen, Z.; Zhao, R. Engineered Tissue Development in Biofabricated 3D Geometrical Confinement−A Review. *ACS Biomater. Sci. Eng.* **2019**, *5* (8), 3688−3702.
(22) Onal, S.; Alkaisi, M. M.; Nock, V. Microdevice-based mechanical compression on living cells. *iScience* **2022**, *25* (12), 105518.
(23) Wang, X.; Gao, Q.; Han, X.; Bu, B.; Wang, L.; Li, A.; Deng, L. Sensitive detection of cell-derived force and collagen matrix tension in microtissues undergoing large-scale densification. *Proc. Natl. Acad. Sci. U.S.A.* **2021**, *118* (36), No. e2106061118.
(24) Hannezo, E.; Heisenberg, C.-P. Rigidity transitions in development and disease. *Trends Cell Biol.* **2022**, *32* (5), 433−444.
(25) Slater, B.; Li, J.; Indana, D.; Xie, Y.; Chaudhuri, O.; Kim, T. Transient mechanical interactions between cells and viscoelastic extracellular matrix. *Soft Matter* **2021**, *17* (45), 10274−10285.
(26) Sun, B. The mechanics of fibrillar collagen extracellular matrix. *Cell Rep. Phys. Sci.* **2021**, *2* (8), 100515.
(27) Barnes, J. M.; Przybyla, L.; Weaver, V. M.; Ewald, A. Tissue mechanics regulate brain development, homeostasis and disease. *J. Cell Sci.* **2017**, *130* (1), 71−82.
(28) Vedadghavami, A.; Minooei, F.; Mohammadi, M. H.; Khetani, S.; Rezaei Kolahchi, A.; Mashayekhan, S.; Sanati-Nezhad, A. Manufacturing of hydrogel biomaterials with controlled mechanical properties for tissue engineering applications. *Acta Biomater.* **2017**, *62*, 42−63.
(29) Traa, W. A.; van Turnhout, M. C.; Nelissen, J. L.; Strijkers, G. J.; Bader, D. L.; Oomens, C. W. J. There is an individual tolerance to mechanical loading in compression induced deep tissue injury. *Clin. Biomech.* **2019**, *63*, 153−160.
(30) Loerakker, S.; Stekelenburg, A.; Strijkers, G. J.; Rijpkema, J. J. M.; Baaijens, F. P. T.; Bader, D. L.; Nicolay, K.; Oomens, C. W. J. Temporal Effects of Mechanical Loading on Deformation-Induced Damage in Skeletal Muscle Tissue. *Ann. Biomed. Eng.* **2010**, *38* (8), 2577−2587.
(31) Kim, J.; Feng, J.; Jones, C. A. R.; Mao, X.; Sander, L. M.; Levine, H.; Sun, B. Stress-induced plasticity of dynamic collagen networks. *Nat. Commun.* **2017**, *8* (1), 842.
(32) Wisdom, K. M.; Adebowale, K.; Chang, J.; Lee, J. Y.; Nam, S.; Desai, R.; Rossen, N. S.; Rafat, M.; West, R. B.; Hodgson, L.; et al. Matrix mechanical plasticity regulates cancer cell migration through confining microenvironments. *Nat. Commun.* **2018**, *9* (1), 4144.
(33) Chaudhuri, O.; Cooper-White, J.; Janmey, P. A.; Mooney, D. J.; Shenoy, V. B. Effects of extracellular matrix viscoelasticity on cellular behaviour. *Nature* **2020**, *584* (7822), 535−546.
(34) Wu, Y.; van der Schaft, D. W. J.; Baaijens, F. P.; Oomens, C. W. J. Cell death induced by mechanical compression on engineered muscle results from a gradual physiological mechanism. *J. Biomech.* **2016**, *49* (7), 1071−1077.
(35) Kalaitzidou, C.; Grekas, G.; Zilian, A.; Makridakis, C.; Rosakis, P.; Rosakis, P. Compressive instabilities enable cell-induced extreme densification patterns in the fibrous extracellular matrix: Discrete model predictions. *PLoS Comput. Biol.* **2024**, *20* (7), No. e1012238.

https://doi.org/10.1021/acsomega.5c00639
ACS Omega 2025, 10, 19675−19681